International Journal of Electronics,
Communication & Instrumentation Engineering
Research and Development (IJECIERD)
ISSN(P): 2249-684X; ISSN(E): 2249-7951
Vol. 4, Issue 2, Apr 2014, 93-106

TRANS STELLAR
• Journal Publications • Research Consultancy

CARRIER FREQUENCY OFFSET ESTIMATOR FOR OFDMA MODE OF WMAN

PUSHPA KOTIPALLI[1], MURALI KRISHNA DOMA[2] & YOGANANDAM YELESWARAPU[3]

[1,2]Department of ECE, Shri Vishnu Engineering College for Women, Bhimavaram, Andhra Pradesh, India

[3]HOD, Department of Electrical Engineering, BITS Pilani, Hyderabad Campus, Andhra Pradesh, India

ABSTRACT

Orthogonal Frequency Division Multiple Access (OFDMA) is proposed in IEEE 802.16e standards for broadband, high data rate fixed/mobile communications. As the basic modulation technique in OFDMA is orthogonal frequency division multiplexing (OFDM), it is severely affected by carrier frequency offset (CFO). The CFO causes loss of orthogonality among the subcarriers. In this paper, we propose a method for estimation of CFO. The proposed method is based on the preamble suggested for OFDMA mode of WMAN where the preamble is loaded on every third subcarrier. The proposed method is an extension of Schimdl and Cox's method. Simulations are conducted for AWGN and frequency selective channels to demonstrate the performance of the proposed method. CRLB for the proposed fractional CFO is derived and is shown that the variance of proposed CFO closely follows CRLB.

KEYWORDS: CFO, Frequency Offset, WMAN, OFDMA, OFDM, CRLB

1. INTRODUCTION

An OFDM system effectively consists of N sinusoidal sub carriers with frequency spacing $1/T$, where T is the active symbol period of each subcarrier. The k^{th} subcarrier will thus be at $f_k=f_0+k/T$, where f_0 is a reference frequency. Without loss of generality, we can assume $f_0=0$. The modulated subcarriers overlap spectrally, but since they are orthogonal over a symbol duration, they can be easily recovered as long as the channel does not destroy the orthogonality. An unwindowed OFDM system has rectangular symbol shapes. Hence, in the frequency domain the individual subchannels will have the form of *sinc* functions. The *sinc* function is defined as

$$\mathrm{sinc}(x) = \frac{\sin(\pi x)}{\pi x} \tag{1}$$

With this definition, it can be confirmed that $sinc(0) = 1$ and that zero crossings occur at ±1, ±2, ±3, …. Since the sine waves existing in each OFDM symbol are truncated every T seconds, the width of the main lobe of the subcarrier *sinc* functions is $2/T$, i.e., there are zero crossings every $1/T$ Hz. and the first side lobe is only 13 dB below the main lobe of the subcarrier [1, 2].

Therefore, N subcarriers can be packed into a bandwidth of N/T Hz, with the tails of the subcarriers trailing off on either side. Since the zero crossings of the frequency domain *sinc* pulses all line up, as long as the frequency offset = 0, there is no interference between the subcarriers. One intuitive interpretation for this is that since the FFT is essentially a frequency-sampling operation, if the frequency offset is negligible, the receiver simply samples received signal at the peak points of the *sinc* functions, where the ICI is zero from all the neighboring subcarriers.

In practice, of course, the frequency offset is not always zero. The major causes for this are mismatched

oscillators at the transmitter and the receiver and Doppler frequency shifts owing to mobility [3]. Since precise crystal oscillators are expensive, tolerating some degree of frequency offset is essential in a consumer OFDM system such as WiMAX. For example, if an oscillator is accurate to 0.1 parts per million (ppm), $f_{\text{offset}} \approx (f_c)(0.1ppm)$. If 3.6 GHz and the Doppler is $f_d=400Hz$, $f_{\text{offset}} \approx (f_c)\ (0.1ppm) + f_d = 760Hz$, which will degrade the orthogonality of the received signal, since now the received samples of the FFT will contain interference from the adjacent subcarriers [4].

Research has shown [5] that the frequency offset error must less than 4% of the OFDM subcarrier interval in AWGN channel and less than 2% of the OFDM subcarrier interval in Rayleigh channel to satisfy the requirement of system synchronization.

If the CFO is several times larger than the subchannel spacing, the offset can be split into an integer part (an integer multiple of the subcarrier spacing) and a fractional part i.e., $\hat{\varepsilon}+\rho$ where ρ represents the integer part of normalized CFO and $\hat{\varepsilon}$ represents the fractional part of normalized CFO. The integer part of the normalized CFO introduces a shift in the subcarrier position at which true data is available. The fractional part of CFO attenuates and phase rotates the symbol on the subcarrier, and also causes inter carrier interference [5]. All these effects of CFO leads to very high bit error rate (BER), sometimes even half of the total data symbols may be in error [6]. To summarize, OFDM is severely affected by carrier frequency offsets. Thus, to mitigate the effects of frequency offset between the transmitter and the receiver, we need to have a very efficient frequency synchronization technique.

CFO estimation techniques may be classified as time-domain (pre-FFT) or frequency domain (post-FFT) techniques. Time-domain methods are generally used to estimate the fractional part of the CFO, although some of these techniques can also estimate the integer part. The post-FFT techniques are usually used to estimate the integer part of the CFO (normalized by the subcarrier spacing) after the fractional part has been identified and corrected.

1.1 Existing CFO Estimators

In order to mitigate frequency offset effect, various techniques have been proposed to estimate the CFO for OFDM systems. The frequency offset mitigation using null symbols is proposed in [7] but the use of a null symbol is not practical in a burst mode system as the transmission will always be a null while no data is transmitted. The self-cancellation schemes were presented in [8] and [9], where the same data is sent in more than one subchannel. These schemes are not very practical as they reduce the number of useful subchannels by at least half. In [5], Moose proposed a maximum likelihood (ML) estimator using repeated data symbol. Although the symbol values need not be known, repetition of OFDM symbols is in essence tantamount to a training-based scheme as it utilizes extra bandwidth. Data-assisted frequency acquisition and tracking were proposed in [10], where periodically inserted known symbols were explicitly used. In [11], Schmidl and Cox proposed a training symbol-based frequency synchronization that utilized an OFDM symbol with identical halves.

This was later generalized to a training symbol with multiple identical parts [12]. Various blind techniques have also been proposed. In [13], Van de Beek et al. developed an ML estimator by exploiting the redundancy in the cyclic prefix (CP). This method, however, is developed based on the nondispersive channel model and suffers the error floor effect in the presence of frequency-selective fading channels. Schmidl and Cox proposed in [14] a blind estimation method that is only suitable to recover CFO values that are multiples of the carrier spacing. In [15-16], Liu and Tureli took advantage of the presence of virtual carriers in OFDM signaling and proposed blind estimation methods reminiscent of

spectral analysis techniques in array processing, i.e., MUSIC and ESPRIT. It was later shown that the proposed MUSIC algorithm is indeed the ML estimate of the CFO with a virtual carrier present signal model [17,18]. The drawback is that it usually requires multiple OFDM symbols to achieve desirable performance, thus introducing an extra delay at the receiver. Tufvesson proposed a frequency offset estimation approach using repeated pseudonoise (PN) sequences [19]. Its estimation range is large. The performance of the time synchronization method using PN sequence is very nice. But there is conflict in choosing the period of PN sequence. Large period of PN sequence means better time synchronization performance, but this will result in smaller range of frequency offset estimation. Now, let us check how far the previous techniques are useful in frame synchronization of OFDMA mode of WMAN.

1.2 Suitability of Existing CFO Estimators in Application to OFDMA Mode of WMAN

To implement CP based frame synchronization algorithm, CP length must be known to the receiver. IEEE 802.16e-2005 [20] standards specify 4 different CPs for OFDMA mode of WMAN. They are 64, 128, 256, and 512. BS selects one CP and transmits the data. As CP is not known to SS, CP based frame synchronization algorithm has to be repeated for all four possible CPs, which is not only time consuming but also laborious task. Also, these algorithms are suitable only for AWGN and very slow fading channels. But, BWA channels based on NLOS propagation are characterized by the stringent multi path delay profile and the fading characteristics. Hence, CP based frame synchronization algorithms are not suitable for OFDMA mode of WMAN.

Preamble based frame detection algorithms depend on the structure of preamble used. Most of these algorithms are based on preamble having two (or four) identical parts, these can be generated by loading on every second (or fourth) subcarrier of the preamble. But IEEE 802.16 standards [20] specify loading on every third subcarrier of the preamble with FFT size 2048 (or 4096) i.e., getting three identical parts is not possible. Hence, preamble based frame detection algorithms too are not suitable for OFDMA mode of WMAN.

Therefore, we have to develop a frequency synchronization algorithm especially for OFDMA mode of WMAN.

This paper is organized as follows. Section 2 presents the proposed method for estimation fractional CFO. CRLB for the proposed fractional CFO is derived in Section 3. Section 4 discusses the estimation of integer frequency offset. Simulation results are provided in Section 5.

2. PROPOSED METHOD FOR FRACTIONAL CFO ESTIMATION

A PN sequence is transmitted along with the OFDMA preamble. For each segment, there are 32 preamble time series [20]. 96 PN sequences are specified for these preamble time series. One out of these 96 known PN sequences is transmitted by BS and the SS has to identify the PN sequence transmitted and cell ID used. Cell ID represents a unique number corresponding to the PN sequence used by the BS. Maximum likelihood estimation [21] can be used to find the PN sequence transmitted. The procedure is as follows: At the receiver, N samples are collected from frame boundary of the received signal sequence. These N received signal samples are correlated with each of the 96 known PN sequences. When the transmitted PN sequence is aligned with receiver PN sequence, a correlation peak is observed. In a multipath channel, the largest correlation peak occurs at the energy peak of the multipath delay profile. Hence frame boundary aligned to the strongest multipath gives the largest correlation peak. The main drawback with this method is that it fails with the presence of frequency offset. It should be applied after frequency compensation. The uncompensated phase difference between signal samples, as a result of frequency offset, will destroy the correlation property of the PN

sequence.We have developed a simple algorithm [22] which can be used for joint estimation of PN sequence and fractional frequency offset. In this algorithm, the PN sequence correlation is robust to frequency offset in the absence of noise.

Let the time domain samples corresponding to the preamble and data symbols be denoted by $x_p(n)$ and $x_d(n)$, respectively. Then, the transmitted signal $x(n)$ can be written as

$$\begin{aligned} x(n) &= x_p(n); \quad 0 \le n \le N+L-1 \\ &= x_d(n); \quad n \ge N+L \end{aligned} \tag{2}$$

The internal block correlation properties of the preamble, discussed in following subsection, are used in development of this algorithm to estimate fractional frequency offset and cell ID. The preamble carrier-sets are defined using the following formula [20]

$$k = n + 3.m \tag{3}$$

Where k denotes indices of subcarriers allocated to a specific sector, n is the index of the carrier-set number (ranging from 0 to 2) and m is a running index from 0 to 567.

Therefore, each sector eventually modulates each third subcarrier. Figure 1 shows three carrier sets corresponding to three sectors. For easy identification, different colors are used for different carrier sets. Subcarrier index 0 corresponds to the first used subcarrier of the preamble (Figure 1). A total of 568 subcarriers at the indices 0, 3, 6, 9,...,1701 form the carrier set for sector 0. Similarly, a total of 568 subcarriers at the indices 1, 4, 7, ..., 1702 form the carrier set for sector 1 where as a total of 567 subcarriers at the indices 2, 5, 8, ..., 1700 form the carrier set for sector2. The used subcarriers in the preamble are modulated using a BPSK modulation with a specific PN sequence. The selection of PN sequence depends on the sector used in the cell [20]. The subsymbols for the guard carriers and dc carrier are zero amplitude symbols.

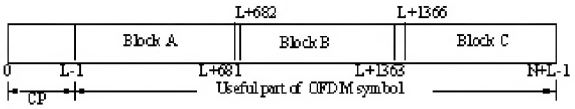

Figure 2: Time Domain Structure for the Preamble in OFDMA Mode of WMAN

Figure 2 shows the block structure for maximum correlation of 496. Let us denote three blocks of 682 samples A_1, B_1, and C_1 representing $a_1(n)$, $b_1(n)$ and $c_1(n)$ respectively as follows.

$$a_1(n) = x_p(n+L); \qquad n = 0,1,...,681 \tag{4}$$

$$b_1(n) = x_p(n+L+683); \qquad n = 0,1,...,681 \tag{5}$$

$$c_1(n) = x_p(n+L+1365); \qquad n = 0,1,...,681 \tag{6}$$

2.1 Proposed CFO Estimator

By following the procedure similar to [21], we estimate the fractional frequency offset and cell ID. In [21], Schmidl and Cox exploited the correlation existing in the two identical parts from the frame boundary of the preamble for the estimation of the fractional frequency offset. Correlation between two identical parts results in energy of one part. But, in the preamble corresponding to OFDMA mode of WMAN, two identical parts do not exist. Instead, this preamble

consists of three correlated blocks as given in (3) to (5). The correlation between any two correlated blocks results in some residual phase. So, Schmidl and Cox method is modified [22], as shown below, to suit the preamble corresponding to OFDMA mode of WMAN.

2.2 Preamble Structure Recommended for OFDMA Mode of WMAN

OFDM modulation with 2048 subcarriers is used in OFDMA mode of WMAN. The first OFDM symbol in downlink of WMAN is the preamble. The preamble is generated with 1702 used carriers, 346 null carriers - 173 on the left, 172 on the right as guard bands and a dc carrier, as shown in Figure 1.

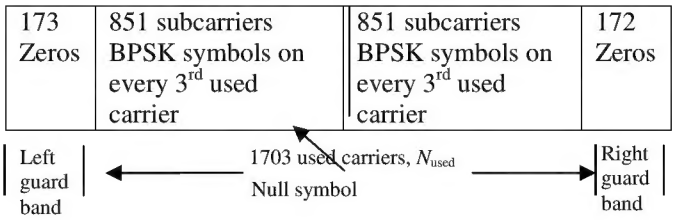

Figure 1: Preamble Subcarriers are Divided into Null Carriers, Dc Carrier and Used Carriers

The cell area corresponding to downlink is divided into three segments and these segments are named as sector 0, sector 1, and sector 2. The used subcarriers are divided into three sets corresponding to the three sectors of the cell.

By multiplying a sample in the block B_1 with corresponding conjugate of a sample in block A_1, we form a reference sequence used for finding correlation. From (3) and (4), the sequence $\nu(n)$ is formed as

$$\nu(n) = a_1^*(n).b_1(n); \qquad n = 0,1,...,681 \tag{6}$$

There are 96 such sequences corresponding to 96 PN sequences specified for OFDMA [20]. Now, the i^{th} correlation sequence, where i = 1, 2,…, 96, is given by

$$\nu^{(i)}(n) = a_1^{(i)*}(n).b_1^{(i)}(n); \qquad n = 0,1,...,681; \tag{7}$$

Where $a_1^{(i)}(n)$ and $b_1^{(i)}(n)$ represent the samples in block A_1 and block B_1 corresponding to the i^{th} PN sequence of the preamble. Substituting (3) and (4) in (7), the i^{th} correlation sequence becomes

$$\nu^{(i)}(n) = x_p^{(i)*}(n+L).x_p^{(i)}(n+L+683); \quad n = 0,1,...,681; \tag{8}$$

To keep the exposition simple, let us assume an ideal channel with no noise. Then, samples of the received signal are given by

$$r(n) = e^{j\left[\frac{2\pi}{N}\varepsilon n+\theta_0\right]}x(n) \tag{9}$$

Here ε represents the CFO between transmitter oscillator and receiver oscillator normalized by subcarrier spacing, given by $\varepsilon = f/\Delta f$ where in Δf is the subcarrier spacing and f is the carrier frequency offset, θ_0 is an initial arbitrary carrier phase, and $\upsilon(n)$ is a zero mean circularly symmetric complex white Gaussian noise with variance σ_υ^2.

From the estimated frame boundary d_{opt}, we find the sequence

$$r'(n) = r^*(d_{opt}+n).r(d_{opt}+L+683);\ \ n=0,1,...,681; \tag{10}$$

We then find the correlation of all sequences $v^{(i)}(n)$, i = 1, 2, …, 96 with $r'(n)$. Substituting (9) in (10), we get

$$r'(n) = x^*(d_{opt}+n).x(d_{opt}+n+683)e^{j\frac{1366\pi\varepsilon}{N}};\ n=0,1,...,681;$$ At $d_{opt} = L$, $r'(n)$ contains the samples of preamble as shown below.

$$r'(n) = x_p^*(L+n).x_p(L+n+683)e^{j\frac{1366\pi\varepsilon}{N}};\ n=0,1,...,681;$$

Now, the PN sequence index corresponding to transmitted PN sequence is given by the value of i corresponding to maximum correlation magnitude [22] i.e.,

$$R_{v,r}(i) = \sum_{n=0}^{681} v_i^*(n).r'(n);\ \ i=1,2,2...,96 \tag{11}$$

$$\text{And } PN_{seq} = \arg\ \max_i \left\{\left|R_{v,r}(i)\right|\right\} \tag{12}$$

Where PN_{seq} is the PN sequence number. Then, unique identification number (cell ID) corresponding to this PN sequence number is obtained. Out of 96 PN sequences [20], first 32 PN sequences correspond to Segment 0, next 32 PN sequences for Segment 1 and the remaining 32 PN sequences correspond to Segment 2. Now depending on the PN sequence number, we can easily identify the Segment selected by the Base station.

Next, let us consider the estimation of frequency offset. The correlation between v^j(n) and r'(n) with maximum magnitude is given by

$$R_{\max} = e^{j\frac{1366\pi\varepsilon}{N}} \sum_{n=0}^{681} \left|x_p(L+n)\right|^2 \left|x_p(L+n+683)\right|^2 \tag{13}$$

Now, the fractional frequency offset is estimated from the angle of $R_{\max}$ as [22]

$$\hat{\varepsilon} = \frac{N}{1366\pi}\angle R_{\max} \tag{14}$$

As every third subcarrier of the preamble is loaded in OFDMA mode of WMAN, the maximum detectable normalized fractional frequency offset becomes $|\hat{\varepsilon}|$ = 1.5. For example, let frequency offset, ε =1.7 is added to the signal at the receiver input. Using this algorithm, we get the estimated frequency offset, $\hat{\varepsilon}$=−1.3. That means, after fractional frequency offset compensation, we observe a subcarrier rotation of 3. This subcarrier rotation is considered as integer frequency offset.

The variance and Cramer Rao Lower Bound (CRLB) of the proposed CFO estimator are derived in the next Section.

3. STATISTICAL ANALYSIS OF THE CFO ESTIMATOR

Theoretical expressions for Variance and Cramer Rao Lower Bound (CRLB) are derived as shown below.

3.1 Variance of the CFO Estimator

Assuming perfect timing synchronization, we have estimated the frequency offset using partial periodic structure present in OFDMA preamble. It is observed from the expression of $r'(n)$ that a pair of samples of two consecutive periodic sections after correlation with transmitted preamble data from a noise free channel will experience a phase offset of $1366\pi/N$. So, phase offset between a pair of periodic sections is obtained from its complex conjugate multiplication. Complex conjugate multiplication of n^{th} sample and $(n + 683)^{th}$ sample can be expressed as

$$r'(n) = r^*(n + d_{opt})r(n + 683 + d_{opt}) \tag{15}$$

When complex conjugate of first sample of useful part of transmitted preamble is multiplied with its 683^{rd} sample we get

$$v(n) = x_p^*(n + L)x_p(n + 683 + L) \tag{16}$$

Considering perfect time synchronization i.e., $d_{opt} = L$, the correlation between $r'(n)$ and $v(n)$ is given by

$$\begin{aligned} z(n) &= v^*(n)r'(n) \\ &= x_p(n + L)x_p^*(n + 683 + L)r^*(n + L)r(n + 683 + L) \end{aligned} \tag{17}$$

Let us consider AWGN channel. Then the received signal can be written as

$$r(n) = e^{j\frac{2\pi}{N}\varepsilon n}x_p(n) + \upsilon(n) \tag{18}$$

Where ε is the normalized frequency offset, and υ is the n^{th} time domain AWGN sample added to OFDMA preamble with mean zero and variance σ_v^2. Substituting (18) in (17), we get

$$\begin{aligned} z(n) = {} & \left|x_p(n + L)\right|^2 \left|x_p(n + L + 683)\right|^2 e^{j\frac{1366\pi\varepsilon}{N}} \\ & + \left|x_p(n + L)\right|^2 x_p(n + L + 683)\upsilon(n + L + 683)e^{-j\frac{2\pi}{N}\varepsilon(n+L)} \\ & + \left|x_p(n + 683 + L)\right|^2 x_p(n + L)\upsilon^*(n + L)e^{j\frac{2\pi}{N}\varepsilon(n+683+L)} \\ & + x_p(n + L)x_p^*(n + L + 683)\upsilon^*(n + L)\upsilon(n + L + 683) \end{aligned}$$

Which can be further written as

$$z(n) = \left|x_p(n + L)\right|^2 \left|x_p(n + L + 683)\right|^2 e^{j\frac{1366\pi\varepsilon}{N}} + \overline{\upsilon(n)} \tag{19}$$

Where $\overline{\upsilon(n)}$ is the effective noise component of the complex conjugate product given by

$$\overline{\upsilon(n)} = \left|x_p(n+L)\right|^2 x_p(n+L+683)\upsilon(n+L+683)e^{-j\frac{2\pi}{N}\varepsilon(n+L)}$$
$$+\left|x_p(n+683+L)\right|^2 x_p(n+L)\upsilon^*(n+L)e^{j\frac{2\pi}{N}\varepsilon(n+683+L)}$$
$$+x_p(n+L)x_p^*(n+L+683)\upsilon^*(n+L)\upsilon(n+L+683)$$

Phase offset estimate $\hat{\phi}(n)$ from the n^{th} sample and $(n+683)^{th}$ sample of the OFDMA preamble may be represented as

$$\hat{\phi}(n) = \frac{1366\pi\varepsilon}{N} + \phi_{noise}(n) \tag{20}$$

Where $\phi_{noise}(n)$ is the phase of the effective noise component $\overline{\upsilon(n)}$. Phase offset $\hat{\phi}$ estimated from pair of M (= 682) samples of the correlated sections present in OFDMA preamble is represented as

$$\hat{\phi} = \frac{1366\pi\varepsilon}{N} + \frac{1}{M}\sum_{n=0}^{M-1}\phi_{noise}(n) \tag{21}$$

Estimated frequency offset $\hat{\varepsilon}$ from the two consecutive correlated sections of the OFDMA preamble can now be written as

$$\hat{\varepsilon} = \varepsilon + \frac{\frac{1}{M}\sum_{n=0}^{M-1}\phi_{noise}(n)}{1366\pi\varepsilon/N} \tag{22}$$

Noise at the n^{th} sample of OFDMA preamble is Gaussian distributed and may introduce a uniformly distributed phase offset of $\pm\pi$ with zero mean and variance $\pi^2/3$. Therefore, variance of frequency offset from (22) may be represented as

$$\text{var}(\hat{\varepsilon}) = \frac{N^2}{3M(1366)^2} \tag{23}$$

Substituting $N = 2048$ and $M = 682$, we get

$$\text{var}(\hat{\varepsilon}) = 1.1\times10^{-3} \tag{24}$$

3.2 CRLB of Estimated CFO

To derive the Cramer Rao Bound of the estimated frequency offset, we rewrite (19) as

$$z(n) = \alpha(n) + j\beta(n) \tag{25}$$

Where $\alpha(n) = A\cos\left(\frac{1366\pi\varepsilon}{N}\right) + \overline{\upsilon_{in}(n)}$ (26)

and $\beta(n) = A\sin\left(\frac{1366\pi\varepsilon}{N}\right) + \overline{\upsilon_{qp}(n)}$ (27)

Where in $A = \left|x_p(n+L)\right|^2 \left|x_p(n+L+683)\right|^2$ (28)

Now, we want to estimate the parameter vector

$$\gamma = [A, \varepsilon]^T \quad (29)$$

The joint probability density function of $z(n)$ can be written as

$$f(z(n);\gamma) = K \exp\left\{\frac{-1}{2\sigma^2}\left[\sum_{n=0}^{M-1}\left((\alpha(n)-\alpha_1(n))^2 + (\beta(n)-\beta_1(n))^2\right)\right]\right\} \text{ where}$$

$$K = \left(\frac{1}{2\pi\sigma^2}\right)^M,\ \alpha_1(n) = A\cos(\phi),\ \beta_1(n) = A\sin(\phi)$$

Where in $\phi = 1366\pi\varepsilon/N$ (30)

Taking the first order partial derivatives of $f(z(n);\gamma)$ with respect to ε yields

$$\begin{aligned}\frac{\partial\left[\ln\left(f(z(n);\gamma)\right)\right]}{\partial\varepsilon} &= \frac{-1}{2\sigma^2}\left[\sum_{n=0}^{M-1}\left((\alpha(n)-A\cos(\phi))^2 + (\beta(n)-A\sin(\phi))^2\right)\right] \\ &= \frac{-1}{2\sigma^2}\sum_{n=0}^{M-1}\left[2(\alpha(n)-A\cos(\phi))(A\sin(\phi))\left(\frac{1366\pi}{N}\right)\right. \\ &\quad \left. +2(\alpha(n)-A\sin(\phi))(-A\cos(\phi))\left(\frac{1366\pi}{N}\right)\right]\end{aligned}$$

Which can be further written as

$$\begin{aligned}\frac{\partial\left[\ln\left(f(z(n);\gamma)\right)\right]}{\partial\varepsilon} &= \frac{-1}{\sigma^2}\left(\frac{1366\pi}{N}\right)\sum_{n=0}^{M-1}\left[(\alpha(n)-A\cos(\phi))(A\sin(\phi))\right. \\ &\quad \left. +(\alpha(n)-A\sin(\phi))(-A\cos(\phi))\right]\end{aligned}$$

Similarly, the second order partial derivative of $f(z(n);\gamma)$ with respect to ε yields

$$\begin{aligned}\frac{\partial^2\left[\ln\left(f(z(n);\gamma)\right)\right]}{\partial\varepsilon^2} &= \frac{-1}{\sigma^2}\left(\frac{1366\pi}{N}\right)^2\sum_{n=0}^{M-1}\left[A^2\sin^2(\phi) + \overline{\upsilon_{in}}A\cos(\phi)\right. \\ &\quad \left. + A^2\cos^2(\phi) + \overline{\upsilon_{qp}}A\sin(\phi)\right]\end{aligned}$$

Which can be further simplified as

$$I(\gamma) = \begin{bmatrix} -E\left\{\frac{\partial^2\left[\ln\left(f(z(n);\gamma)\right)\right]}{\partial A^2}\right\} & -E\left\{\frac{\partial^2\left[\ln\left(f(z(n);\gamma)\right)\right]}{\partial A\partial\varepsilon}\right\} \\ -E\left\{\frac{\partial^2\left[\ln\left(f(z(n);\gamma)\right)\right]}{\partial A\partial\varepsilon}\right\} & -E\left\{\frac{\partial^2\left[\ln\left(f(z(n);\gamma)\right)\right]}{\partial\varepsilon^2}\right\} \end{bmatrix}$$

Now, the variance of the fractional CFO estimator is

$$var(\hat{\varepsilon}) \geq \frac{1}{I(\gamma)_{II}} = \frac{1}{E\left\{\frac{\partial^2[\ln(f(z(n);\gamma)]}{\partial\varepsilon^2}\right\}} = \frac{\sigma^2}{\left(\frac{1366\pi}{N}\right)^2 MA^2} = \frac{N^2}{(1366\pi)^2 M(SNR)} \tag{31}$$

Where $SNR = \frac{A^2}{\sigma^2}$ (32)

Therefore, the Cramer Rao Lower Bound (CRLB) for the variance of frequency offset estimation is given as

$$\left(\text{var}(\hat{\varepsilon})\right)_{CRLB} = \frac{N^2}{(1366\pi)^2 M(SNR)} \tag{33}$$

Substituting $N = 2048$ and $M = 682$, we get the CRLB for the variance of estimated frequency offset as

$$\left(\text{var}(\hat{\varepsilon})\right)_{CFRLB} = \frac{3.3394\times10^{-4}}{SNR} \tag{34}$$

4. SIMULATION RESULTS

In our simulation, a wireless system operating at 3.6GHz and with bandwidth of 20MHz is assumed. Three channel scenarios are considered: an AWGN channel, time-invariant NLOS Rayleigh fading channels (SUI-2, SUI-4 and SUI-6), and time-variant Rayleigh fading channels (3GPP Ped-B and 3GPP Veh-A) with the Maximum Doppler Shift 400 Hz. The simulation parameters of OFDMA system given in Table 1 are used. The preamble is generated with subcarrier loading as shown in Figure 1. Every third used carrier is loaded with PN sequence corresponding to Sector = 0 and cell ID = 10 [20]. A frequency offset of 1.7 times the subcarrier spacing is assumed in the simulations. For this frequency offset, the estimated fractional frequency should be $\hat{\varepsilon} = -1.3$. In what follows, we analyze the performance of the proposed fractional CFO estimator.

Table 1: Simulation Parameters of OFDMA System

Parameter	Value
Channel Bandwidth, BW	20 MHz
Oversampling rate n = F_s/BW	28/25
Sampling Frequency F_s = floor(*n.BW*/8000)×8000	22.4 MHz
No. of Total Subcarriers, *N*	2048
Subcarrier Spacing $\Delta f = F_s/N$	10.94 KHz
Useful Symbol Time $\Delta T_s = 1/\Delta f$	91.43 µs
Guard Time $Tg = G.T_s$	22.86, 11,43, 5.7, 2.86 µs
Left Guard Band	Zeros are loaded on left 173 subcarriers
Right Guard Band	Zeros are loaded on left 172 subcarriers
Modulation (Preamble)	BPSK on every third subcarrier
Modulation (Data Symbols)	QPSK

Table 1: Contd.,

Carrier Frequency	3.6 GHz
MS Velocity	30 kmph for 3GPP Ped B 120 kmph for 3GPP Veh A
Max. Doppler Frequency	100 Hz for 3GPP Ped B 400 Hz for 3GPP Veh A
Number of Cells	3

4.1 Performance of Fractional CFO

To illustrate how the frequency offset estimation algorithm performs in both AWGN and frequency selective channels, we have performed simulations with 1000 different realizations of channel and noise. SUI channel models (for fixed WMAN) [23] and 3GPP channel models (for mobile WMAN) [24] are used to test the proposed methods in frequency selective channels. f_dT = 0.04 is considered in 3GPP channel model. The impulse response of the channel is normalized to unit norm. From the results of 1000 realizations, we computed mean and variance of the fractional frequency offset estimate considering frame boundary along the strongest path of the channel. The computed values of mean and variance of the fractional frequency offset are tabulated in Table 2. Table 2 shows that for AWGN as well as frequency selective channels, as SNR increases from 0 dB to 10 dB, the error in mean value decreases. At SNR = 10 dB, 3GPP Pedestrian-B channel exhibits largest error variance. The second largest error variance is exhibited by SUI-4 channel. The high error variance exhibited by 3GPP Pedestrian-B and SUI-4 channels is due their bad power profiles as compared to all other frequency selective channels. Remaining channels - AWGN, SUI-2, SUI-4 and 3GPP Vehicular-A channels exhibit more or less similar error variance. Combining the results of low error variance of frequency selective channels with the results of mean, we observe that the fractional CFO estimate is very close to the true value.

Table 2: Mean and Variance of the Fractional CFO Estimate $\hat{\varepsilon}$ (the Actual Normalized CFO, ε = 1.4)

S. No.	Channel Type	SNR	Fractional CFO Estimate	
			Mean	Variance
1.	AWGN	0 dB	1.3972	0.7189×10^{-3}
		10 dB	1.3988	0.0558×10^{-3}
2.	SUI - 2	0 dB	1.3957	0.4577×10^{-3}
		10 dB	1.3985	0.0559×10^{-3}
3.	SUI - 4	0 dB	1.4027	0.5002×10^{-3}
		10 dB	1.4003	0.0629×10^{-3}
4.	SUI - 6	0 dB	1.4027	0.4714×10^{-3}
		10 dB	1.4002	0.0530×10^{-3}
5.	Ped - B	0 dB	1.4066	0.5780×10^{-3}
		10 dB	1.4027	0.0952×10^{-3}
6.	Ped - A	0 dB	1.3985	0.4644×10^{-3}
		10 dB	*1.3991*	*0.0507×10^{-3}*

We repeated the experiment for different values of SNR. 1000 different channel and noise realizations are conducted at each SNR value with SNR ranging from 0 dB to 40 dB in steps of 5 dB. A frequency offset of 1.4 times the subcarrier spacing is assumed in the simulations. Figure 3 and Figure 4 show the mean and variance of fractional CFO estimator over different SNR values when frame boundary is considered along the strongest path of the channel. These plots show that the fractional CFO estimator shows less deviation of mean from the true value, even in the presence of high doppler channels like 3GPP Pedestrian-B and Vehicular-A channels. And also, the proposed fractional CFO estimator exhibits more or less similar performance in all channels and yields good results even at SNR = 0 dB.

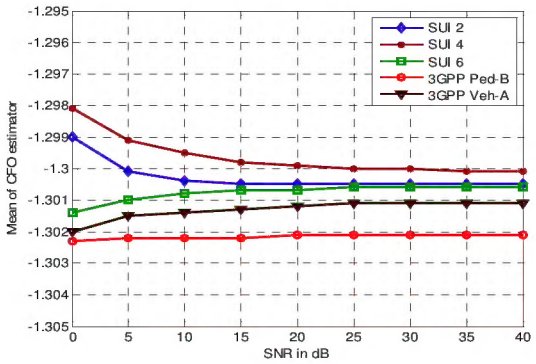

Figure 3: Mean of Fractional CFO Estimate (Normalized CFO, ε =1.4, Frame Boundary is Considered along Strongest Path of the Channel, and f_Dt=0.04)

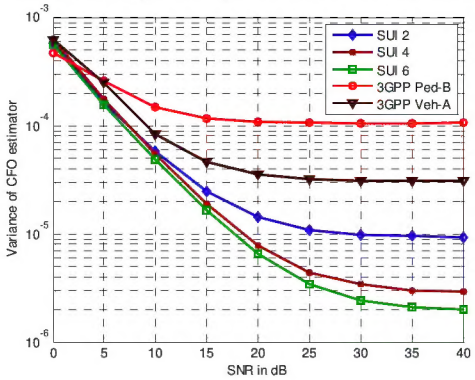

Figure 4: Variance of Fractional CFO Estimate (Normalized CFO, ε =1.4, Frame Boundary is Considered along Strongest Path of the Channel, and f_Dt=0.04)

From Figure 4, we note that the variance CFO estimate increases as frequency selectivity increases. The channel dispersion length of Pedestrian-B channel is large as compared to Vehicular-A channel and also, its second channel tap amplitude is largest among all. This causes high error variance. Therefore, the variance of fractional CFO estimator with 3GPP Pedestrian-B channel is more than that of 3GPP Vehicular-A channel. In the similar way, the variance of SUI-4 channel is more than that of SUI-6 channel. In this case the bad power profile of SUI-4 increases the error variance of the CFO estimator. If we compare frequency selective channels, SUI-2 channel, due to its line of sight component, exhibits least minimum error variance.

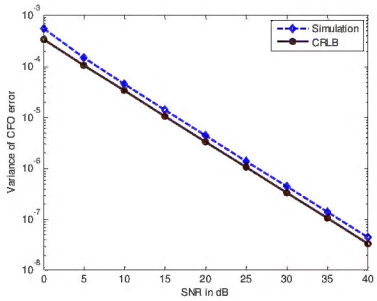

Figure 5: Variance of Fractional CFO Estimate in Comparison to its CRLB (Normalized CFO, ε =1.4, Frame Boundary is Considered along Strongest Path of the Channel)

From Figure 5, we note that the error variance of proposed CFO estimator in AWGN closely follows the CRLB plot.

5. CONCLUSIONS

In this paper, we proposed a method for joint estimation of fractional CFO for OFDMA mode of WMAN. Error Variance and CRLB of the proposed CFO estimator are derived. Simulations are conducted for AWGN and frequency selective channels to demonstrate the performance of the proposed method. It is found that the error variance of proposed CFO estimator in AWGN closely follows the CRLB plot. Also, the estimated fractional CFO is very close to the true value for both AWGN and frequency selective channels.

REFERENCES

1. OPPENHEIM, A.V., SCHAFER, R.W (1999), *Discrete-Time Signal Processing*, 2nd ed. Prentice-Hall, ISBN 0–13–083443–2.
2. J.G. PROAKIS AND D.G. MANOLAKIS (1996), *Digital Signal Processing: Principles, Algorithms, and Applications,* 3rd ed. Prentice Hall, ISBN: 0–13–373762–4.
3. T. POLLET, M. VAN BLADEL, AND M. MOENECLAEY (1995), *BER sensitivity of OFDM systems to carrier frequency offset and Wiener phase noise,* IEEE Trans. Commu., vol. 43, no. 234, pp. 191–193.
4. JEFFREY G. ANDREWS, ARUNABHA GHOSH, RIAS MUHAMED (2007), *Fundamentals of WiMAX: Understanding Broadband wireless Networking*, Prentice Hall.
5. P. H. MOOSE (1994), *A technique for orthogonal frequency division multiplexing frequency offset correction*, IEEE Trans. Commun., vol. 42, pp. 2908-2914.
6. L. HANZO et. al. (2003), *OFDM and MC-CDMA for broadband multi user communications, WLANs and broadcasting*, IEEE Press.
7. H. NOGAMI AND T. NAGASHIMA (1995), *A frequency and timing period acquisition technique for OFDM systems*, in Proc. IEEE PIRMC, pp. 1010–1015.
8. J. ARMSTRONG (1999), *Analysis of new and existing methods of reducing inter carrier interference due to carrier frequency offset in OFDM*, IEEE Trans. on Commun, vol. 47, pp. 365–369.
9. Y. ZHAO AND S.G. HAGGMAN (2001), *Inter carrier interfernce self-cancellation scheme for OFDM mobile communication systems*, IEEE Trans. Commun., vol. 49, pp. 1185–1191.
10. M. LUISE AND R. REGGIANNINI (1996), *Carrier frequency acquisition and tracking for OFDM systems*, IEEE Trans. Commun., Vol. 44, pp. 1590–1598.
11. T.M. SCHMIDL AND D.C. COX (1997), Robust frequency and timing synchronization for OFDM, IEEE Trans. Commun., vol. COM–45, pp. 1613–1621.
12. M. MORELLI AND U. MENGALI (1999), *An improved frequency offset estimator for OFDM applications*, IEEE Commun. Lett., Vol. 3, pp. 75–77.
13. J.J. VANDE BEEK, M. SANDELL AND P.O. BORJESSON (1997), *ML estimation of time and frequency offset in OFDM systems*, IEEE Tran. Signal Processing, vol. 45, pp. 1800–1805.

14. T.M. SCHMIDL AND D.C. COX (1997), *Blind synchronization for OFDM*, Electron. Lett., Vol. 33, pp. 113–114.

15. H. LIU AND U. TURELI (1998), *A high–efficiency carrier estimator for OFDM communications*, IEEE Commun. Lett., Vol. 2, pp. 104–106.

16. U. TURELI, H. LIU, AND M. ZOLTOWSKI (2000), *OFDM blind carrier offset estimation: ESPRIT*, IEEE Trans. Commun., Vol. 48, pp. 1459–1461.

17. X. MA AND G.B. GIANNAKIS (2001), *Unifying and optimizing null-subcarrier based frequency-offset estimators for OFDM*, in Proc. Int. Conf. Inform, Commun., Signal Process., Singapore.

18. M. GHOGHO, A. SWAMI, AND G.B. GIANNAKIS (2001), *Optimizing null-subcarrier selection for CFO estimation in OFDM over frequency-selective fading channels*, in Proc. GLOBECOM.

19. F. TUFVESSON, M. FAULKNER, AND O. EDFORS (1999), *Time and frequency synchronization for OFDM using PN sequence preambles*, in Proceedings of IEEE Veh. Tech. Conf., pp. 2203–2207.

20. *Part 16: Air interface for fixed and mobile broadband wireless access systems*, IEEE std. 802.16e-2005.

21. JOHN G. PROAKIS (2001), *Digital Communications*, 4th ed., McGraw–Hill International Edition.

22. K. PUSHPA, CH. N. KISHORE AND Y. YOGANANDAM (2008), *Estimation of Frequency Offset, Cell ID and CP Length in OFDMA mode of WMAN*, IEEE Intl.Conf. TENCON 2008, 18–21.

23. IEEE 802. 16 BWA WORKING GROUP, *Channel Models for Fixed Wireless Applications*, IEEE 802. 16. 3c-01/29r4, http://ieee802. org/16, 2001-07-16.

24. RAJ JAIN (2007), *Channel Models: A Tutorial*, V1. 0, February 21.